Alternating iteration method in multi-connected crack interactions

C. K. Chen[1]

Summary

A classical alternating iteration method is applied to evaluate the stress intensity factors for a mixed oriented crack approaching semi-infinite plane or a straight crack. Conventional Gaussian-Legedre quadrature scheme is employed for the numerical integration in the crack vs. free boundary interacting problems; however, averaged image stresses along crack surfaces are invoked to simplify the alternating procedures in crack vs. crack interaction. Good correlation was achieved between the iterated solutions and the available solutions in the literature. As crack approach the free semi-infinite plane, mode I affect increases, however, maximum mode II stress intensity factors may shift to the lower angle from its original extreme with slant angle of $45°$. In the interaction between cracks, the stress intensity factor of straight crack is enhanced for closely located cracks with a crack of aligned angle in the range of $\beta = 0° \sim 20°$. Nevertheless, close proximity may jeopardize the numerical convergence in the alternating iteration due to the inadequacy of conventional integration scheme in dealing with numerical singularities.

keywords: Multi-Connected Domains, Crack, Semi-Infinite Plane, Stress Intensity Factors, Mechanics of Fracture

Introduction

Progress in the understanding of fracture has long been limited by incomplete mathematical descriptions of conditions prevailing near a crack tip, particularly in ductile materials. The techniques of mathematical formulation for crack problem have received increasing amounts of attention from researchers in recent years, and some important advances have been made [1]. The multiple-connected crack problem is a special branch in mechanics of fracture. Nevertheless, such conditions occasionally occur in the real world, e.g., multiple-crack on surface of pressure vessels, transmission pipelines, and underneath crack in rail track etc., due to severe stress corrosion or thermal fatigue or fretting fatigue.

A region is simply connected if any simple closed contour drawn in the region can be shrunk continuously to a point without leaving the region, otherwise the region is said to be multiply connected. As illustrates in Fig. 1(a), a simple connected domain D in which an arbitrary closed curve C can be shrunk continuously to a point without leaving D. Green's theorem states that

$$\oint_C (Pdx + Qdy) = \iint_D \left(\frac{\partial Q}{\partial x} - \frac{\partial P}{\partial y} \right) dxdy \tag{1}$$

---

[1]Department of Mechanical Engineering, Cheng Shiu University. E-mail: joss@csu.euu.tw
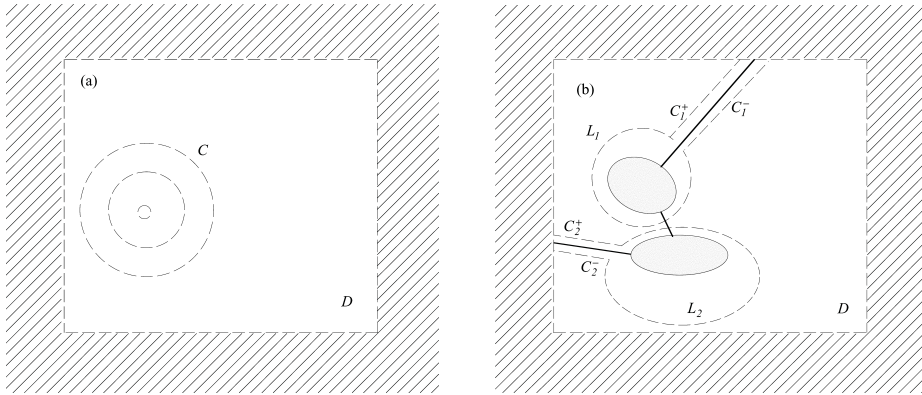
Figure 1: 2-D examples of simply and multiply connected domains (a) simply connected domain (b) multiply connected domain

where P and Q are analytic function in the plane of $x - y$ bounded by a closed contour C. When the condition

$$\frac{\partial Q}{\partial x} - \frac{\partial P}{\partial y} = 0 \tag{2}$$

is imposed, the line integral on the left side of Eq. (1) vanishes for every possible closed contour C. The condition assures single-valuedness of the integral in single connected domain. This exact differential of Eq. (1) provides the necessary and sufficient compatibility in the displacement fields to be single-valuedness in a simply connected domain. Fig. 1(b) present multiply connected domains in which $L's$ are integrating contours and simply connected can be made by introducing cuts i.e., imaginary boundary which are displayed as broader lines in Fig. 2 (b). For a multiply connected domain the displacement compatibility may be necessary but no longer be sufficient. To guarantee single-valuedness of displacement for an assumed strain field, some auxiliary conditions shall be imposed. An $(m + 1)$-ply connected region can be made simply connected by using m cuts. In the cut, simple connected region, m independent simple contours $L_1, L_2, \cdots, L_m$ can be drawn. Each L_i starts from one side of a cut, and ends on the other side of the same cut. All cuts are thus embraced by the $L's$. Then single-valuedness for displacement field can be assure by imposing m supplementary conditions in Eq.(2.40).

$$\oint_{L_1} (Pdx + Qdy) = \oint_{L_2} (Pdx + Qdy) = \cdots = \oint_{L_m} (Pdx + Qdy) = 0 \tag{3}$$

Since only simply connected domains can be mapped conformally on a circle in a one-to-one manner, the multiply connected domains problems need special

considerations. However, in the multiply connected domains, there retains a simple relation between mapping function and the Green's function. As Green's function can be constructed for multiple connected domains, that at once suggests a generalization of the integral equation approach. One such generalization has been made by Mikhlin [2] who reduced the basic problems of plane elasticity in multiply connected domains to the solution of certain Fredholm integral equations which are described by the kernels depend on Green's functions. Although Mikhlin's equations serve admirably to establish the existence of solutions in multiply connected domains, they possess the disadvantage of being dependent on the solution of an auxiliary Dirichlett's problem for Green's function. It is essentially desirable to formulate the relevant auxiliary equations which are account for the given boundary conditions.

Semi-infinite boundaries, interfaces, and material imperfections (such as voids, inclusions and dislocations) interacting with cracks may play important roles in the understanding of fracture behavior in solids. Considerable attentions had been received for the last few decades in this subject [3]. Mathematically speaking, these interacting crack problems are within the topic of multi-connected regions in solid mechanics. Many investigators had developed certain methods in evaluating crack interaction problems, namely, pseudo-tractions methods [4], Laurent series expansion [5], body force method [6] and integral transform [7]. These analyses are conducted by formulating the complex stress functions and tailored the crack face tractions to yield the correct net tractions for the overall problems. Most versions have employed truncated polynomial series to expand the crack-face tractions, where polynomial coefficients are found from a large system of linear algebraic equations. Nevertheless, another powerful approach known as the distributed dislocation technique formulates crack interaction problems in terms of singular integral equations with Cauchy kernels. Common solutions are utilized Gauss-Chebyshev quadrature to obtain crack tip stress intensity factors. In addition, a monograph by Hills et al [8] describes in detail for this distributed dislocation technique.

Schwarz's Alternating Method

Since elastostatic problems in multiply connected domains request serious computational difficulties, it is natural to attempt to reduce their solutions in terms of sequence of problems in simple connected regions. The multiply connected domains is displayed in Fig. 2, where the overlapping domains R_1 and R_2 each of which is bounded by simple close contours C_1 and C_2. Let the portion of the contour C_1 bounding R_1 lay within the region R_2 be C_1' and the part outside R_2 be C_1". Then $C_1 = C_1' + C_1$". The similar denotation is appled to contour C_2 respectively. The region R_{12} that is common to R_1 and R_2 is thus bounded by C_1' and C_2', while the region $R_1 + R_2$ has the enclosed curve C_1"$+C_2$" for its boundary. Schwarz achieved
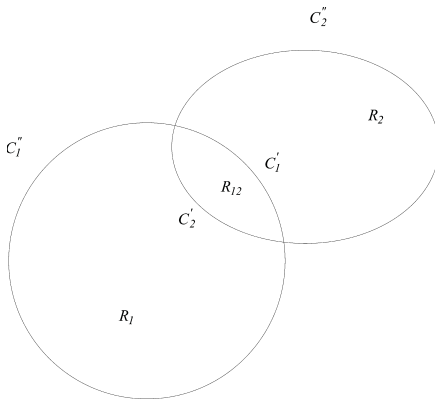
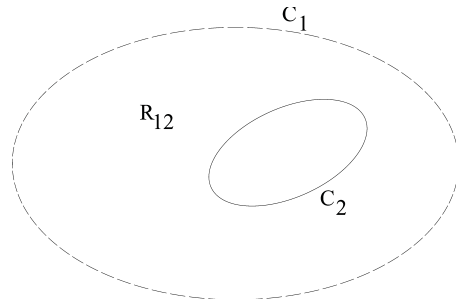Figure 2: Overlapping of doubly connected region

Figure 3: Intersection of doubly connected region

the solution of Dirichlet problems by the superposition of a sequence of solutions in simply connected domains. This treatment was called by himself namely the alternating method [9]. This method can achieve whether the desired solution or not mainly rely on the properties of the governing operator and the nature of assigned boundary values. For Dirichlet problems, the governing operator is Laplacian and the values defined on smooth boundary of the domain are continuous, and thus Schwarz treatment yield the desired solution.

We now consider the Schwarz method for he doubly connected elastostatic problem, where the operator is $L(\phi,\varphi)$ and the boundary condition on $C_1 + C_2$ is $L(\phi(t),\,\varphi(t)) = f(t)$. To obtain the first approximation $\left(\phi^{(1)},\varphi^{(1)}\right)$ to (ϕ,φ), We can determine the approximated function $\phi^{(1)},\varphi^{(1)}$ in region R_1 so that

$$L\left(\phi^{(1)},\varphi^{(1)}\right)_{C_1} = f(t)_{C_1'} \qquad (4)$$

To get the second approximation $\left(\phi^{(2)},\varphi^{(2)}\right)$, the solution in R_2 is accomplished and that

$$L\left(\phi^{(2)},\varphi^{(2)}\right)_{C_2} = f(t)_{C_2} - L\left(\phi^{(1)},\varphi^{(1)}\right)_{C_2'} \qquad (5)$$

For the third approximation, the estimated solution in region R_1 can be assumed as

$$L\left(\phi^{(3)},\varphi^{(3)}\right)_{C_1} = f(t)_{C_1} - L\left(\phi^{(2)},\varphi^{(2)}\right)_{C_1'} \qquad (6)$$

and so forth. It was observed by Neumann that Schwarz method can be modified to complete the solution for the domain R_{12} where R_{12} is the intersection of R_1 and R_2.
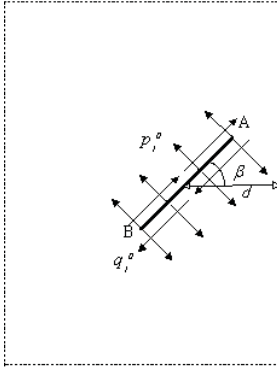
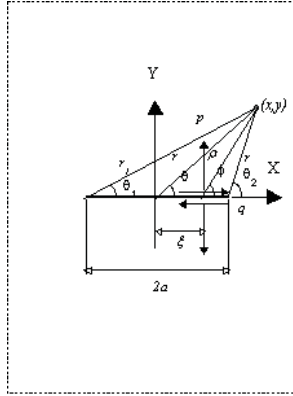Figure 4: Schematic drawing of a slant crack interacts with half plane

Figure 5: Geometric representation for a crack with a pair of split normal and shear forces on the crack face
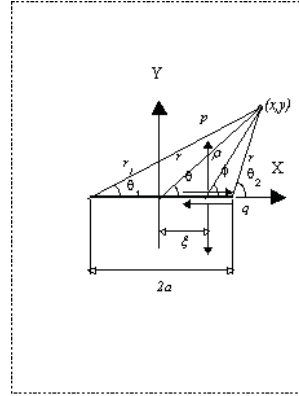
Figure 6: Geometric representation for a semi-infinite plane with split normal and shear forces on its face

As it is depicted in Fig. 3 for doubly connected domain, the intersection region R_{12} is formed by the infinite region R_1 bounded by C_1 with the finite region R_2 interior to C_2.

Interactions of Crack vs. Semi-infinite

As denoted in the Schwarz's alternating iteration algorithm, fundamental analytic solution is essentially required for each simply connected region respectively. For the interacting problem of free semi-infinite plane and an internal crack illustrated in Fig. 4, analytical solutions for the crack and semi-infinite plane with a concentrated pair of tensile and shear force demonstrated in Fig. 5 and 6 shall be recognized in a prior in order to evaluate the interaction outcome in this interacting question.

The Westergaard function is a powerful semi-inverse method for solving problems of plane elasticity with cracks. In addition, the Westergaard functions Z_I and Z_{II} with split concentrated tensile force p and shear force q denoted in Fig. 5 can be found as

$$\left\{\begin{matrix} Z_I \\ Z_{II} \end{matrix}\right\} = \frac{1}{\pi} \left\{\begin{matrix} p \\ -iq \end{matrix}\right\} \frac{\sqrt{a^2 - \xi^2}}{(z - \xi)\sqrt{z^2 - a^2}} \tag{7}$$

where a is the half crack length, ξ gs the position that the split forces applied, and the distance $z=x+iy$ is measured from the center of the crack. Following the imple-

mentation of Westergaard functions, the stress field can be derived as

$$
\begin{aligned}
\sigma_x &= \left[Re\left(Z_I\right) - yIm\left(Z_I'\right)\right] + \left[2Re\left(Z_{II}\right) - yIm\left(Z_{II}'\right)\right] \\
\sigma_y &= \left[Re\left(Z_I\right) + yIm\left(Z_I'\right)\right] + \left[yIm\left(Z_{II}'\right)\right] \\
\tau_{xy} &= \left[-yRe\left(Z_I'\right)\right] + \left[-Im\left(Z_{II}\right) - yRe\left(Z_{II}'\right)\right]
\end{aligned}
\tag{8}
$$

$$
F_x = \frac{1}{\pi\rho}\sqrt{\frac{a^2 - \xi^2}{r_1 r_2}}\left\{\cos\left(\phi + \frac{\theta_1 + \theta_2}{2}\right)\right.
$$
$$
\left. - \frac{y}{\rho}\left[\sin\left(2\phi + \frac{\theta_1 + \theta_2}{2}\right) + \frac{r\rho}{r_1 r_2}\sin\left(\phi - \theta + \frac{3\left(\theta_1 + \theta_2\right)}{2}\right)\right]\right\}
$$

$$
G_x = -\frac{1}{\pi\rho}\sqrt{\frac{a^2 - \xi^2}{r_1 r_2}}\left\{2\sin\left(\phi + \frac{\theta_1 + \theta_2}{2}\right)\right.
$$
$$
\left. + \frac{y}{\rho}\left[\cos\left(2\phi + \frac{\theta_1 + \theta_2}{2}\right) + \frac{r\rho}{r_1 r_2}\cos\left(\phi - \theta + \frac{3\left(\theta_1 + \theta_2\right)}{2}\right)\right]\right\}
$$

$$
F_y = \frac{1}{\pi\rho}\sqrt{\frac{a^2 - \xi^2}{r_1 r_2}}\left\{\cos\left(\phi + \frac{\theta_1 + \theta_2}{2}\right)\right.
$$
$$
\left. + \frac{y}{\rho}\left[\sin\left(2\phi + \frac{\theta_1 + \theta_2}{2}\right) + \frac{r\rho}{r_1 r_2}\sin\left(\phi - \theta + \frac{3\left(\theta_1 + \theta_2\right)}{2}\right)\right]\right\}
$$

$$
G_y = \frac{y}{\pi\rho^2}\sqrt{\frac{a^2 - \xi^2}{r_1 r_2}}\left[\cos\left(2\phi + \frac{\theta_1 + \theta_2}{2}\right) + \frac{r\rho}{r_1 r_2}\cos\left(\phi - \theta + \frac{3\left(\theta_1 + \theta_2\right)}{2}\right)\right]
$$

$$
F_{xy} = \frac{y}{\pi\rho^2}\sqrt{\frac{a^2 - \xi^2}{r_1 r_2}}\left[\cos\left(2\phi + \frac{\theta_1 + \theta_2}{2}\right) - \frac{r\rho}{r_1 r_2}\cos\left(\phi - \theta + \frac{3\left(\theta_1 + \theta_2\right)}{2}\right)\right]
$$

$$
G_{xy} = \frac{1}{\pi\rho}\sqrt{\frac{a^2 - \xi^2}{r_1 r_2}}\left\{\cos\left(\phi + \frac{\theta_1 + \theta_2}{2}\right)\right.
$$
$$
\left. - \frac{y}{\rho}\left[\sin\left(2\phi + \frac{\theta_1 + \theta_2}{2}\right) + \frac{r\rho}{r_1 r_2}\cos\left(\phi - \theta + \frac{3\left(\theta_1 + \theta_2\right)}{2}\right)\right]\right\}
\tag{9}
$$

in which Z' is dZ/dz, and Re and Im denote the corresponding real and imaginary parts of the complex potential. Nevertheless, the explicit depiction of this stress field can be presented in polar coordinate system [10], i.e. $z = re^{i\theta}$, and the resulting explicit stress fields are shown in Eq. (9) and (10) where geometric parameters are referred to Fig. 5.

$$\sigma_x^c = pF_x(a, r_1, r_1, \rho, \theta_1, \theta_2, \phi, \xi) + qG_x(a, r_1, r_1, \rho, \theta_1, \theta_2, \phi, \xi)$$
$$\sigma_y^c = pF_y(a, r_1, r_1, \rho, \theta_1, \theta_2, \phi, \xi) + qG_y(a, r_1, r_1, \rho, \theta_1, \theta_2, \phi, \xi) \qquad (10)$$
$$\tau_{xy}^c = pF_{xy}(a, r_1, r_1, \rho, \theta_1, \theta_2, \phi, \xi) + qG_{xy}(a, r_1, r_1, \rho, \theta_1, \theta_2, \phi, \xi)$$

Considering the stress field in semi-infinite plane of Fig. 6, there exists a basic solution called the simple radial distribution or Boussinesq solution [11]. This analytic solution is well known in the field of contact mechanics. However, the stress field owing to a corresponding concentrated normal and shear fore is depicted in Eq.(11)-(12).

$$\sigma_x^c = pM_x + qN_x$$
$$\sigma_y^c = pM_y + qN_y \qquad (11)$$
$$\tau_{xy}^c = pM_{xy} + qN_{xy}$$

$$M_x = \frac{2x^3}{\pi \left[x^2 + (y - \eta)^2 \right]^2}, \quad N_x = -\frac{2x^2 (y - \eta)}{\pi \left[x^2 + (y - \eta)^2 \right]^2}$$

$$M_y = \frac{2x(y - \eta)^2}{\pi \left[x^2 + (y - \eta)^2 \right]^2}, \quad N_y = -\frac{2(y - \eta)^3}{\pi \left[x^2 + (y - \eta)^2 \right]^2} (12) \qquad (12)$$

$$M_{xy} = \frac{2x^2 (y - \eta)}{\pi \left[x^2 + (y - \eta)^2 \right]^2}, \quad N_{xy} = -\frac{2x(y - \eta)^2}{\pi \left[x^2 + (y - \eta)^2 \right]^2}$$

Consider the interacting problem shown in Fig 7(a), Büeckner's superposition principle can be applied to access the stress intensity factors at both tip of the inclined crack. The original problem can be decomposed in to two subproblems as demonstrated in Fig. 7(b) and 7(c). The traction components (p_1^0, q_1^0, p_2^0 and q_2^0) on the crack surface and semi-infinite plane can be derived as

$$\begin{cases} p_1^0 = \sigma^\infty \cos^2 \beta, & q_1^0 = \sigma^\infty \sin \beta \cos \beta \\ p_2^0 = 0, & q_2^0 = 0 \end{cases} \qquad (13)$$

The subproblems can be solved when each boundary is considered as isolation and loaded by unknown tractions including interaction effects. Two subproblems of
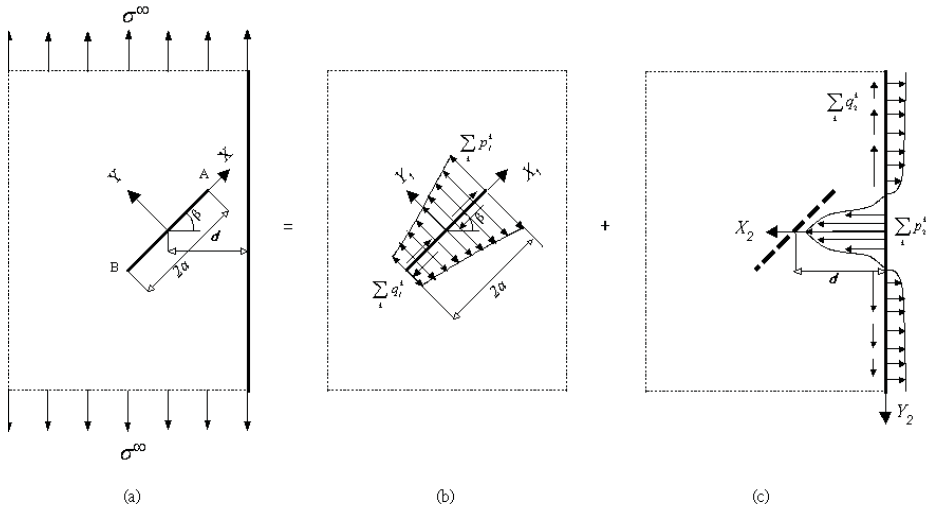
Figure 7: Bückner's superposition for a internal crack interacts with half plane

Fig. 7(b) and Fig. 7(c) can now be appropriately solved by alternating iteration method, and are thus resolved respectively to free its own boundary tractions. In each loading system, stress distributions on the imaginary position of cracks are calculated with corresponding stress functions in Eq. (10) and Eq. (11) where Green function characteristics can be easily applied for the corresponding stress field with distributed loading. They are denoted as

$$
\begin{cases}
\sigma_x = \int\limits_{-a}^{a} [p(\xi)F_x + q(\xi)G_x]d\xi \\
\sigma_y = \int\limits_{-a}^{a} [p(\xi)F_y + q(\xi)G_y]d\xi \\
\tau_{xy} = \int\limits_{-a}^{a} [p(\xi)F_{xy} + q(\xi)G_{xy}]d\xi
\end{cases}
\tag{14}
$$

$$
\begin{cases}
\sigma_x = \int\limits_{-\infty}^{\infty} [p(\eta)M_x + q(\eta)N_x]d\eta \\
\sigma_y = \int\limits_{-\infty}^{\infty} [p(\eta)M_y + q(\eta)N_y]d\eta \\
\tau_{xy} = \int\limits_{-\infty}^{\infty} [p(\eta)M_{xy} + q(\eta)N_{xy}]d\eta
\end{cases}
\tag{15}
$$

Whereas only one boundary exists in each iterating cycle, the remaining boundary is considered as an imaginary boundary. The stress field with negative traction on each imaginary boundary is then imposed onto the existing stress field to free boundary traction. In doing so, new image traction may be introduced to the once image traction free boundary. These remaining image tractions are successively

reduced by the repeated alternating iteration. A similar process is repeated until the remaining image traction on both boundaries approach zero simultaneously. There is an obvious advantage to this iteration method, in which the interaction effect between boundaries has been particularly considered. The image tractions on the free surfaces of the prospective crack can then be collected in every iteration cycle. Therefore, the kth increment of stress intensity factors at crack tip () owing to mutual boundaries interaction can be integrated from the concentrated force results provided in Tada et al [12] and display in Eq. (10), where and are the normal and shear image stresses function distributed along the crack in the kth iteration.

$$\Delta K_I^k(\pm a) = \frac{1}{\sqrt{\pi a}} \int_{-a}^{a} p_1^k(x_1) \sqrt{\frac{a \pm x_1}{a \mp x_1}} dx_1$$

$$\Delta K_{II}^k(\pm a) = \frac{1}{\sqrt{\pi a}} \int_{-a}^{a} q_1^k(x_1) \sqrt{\frac{a \pm x_1}{a \mp x_1}} dx_1$$

(16)

Therefore the stress intensity factors at the crack tips are

$$\begin{Bmatrix} K_I(\pm a) \\ K_{II}(\pm a) \end{Bmatrix} = \begin{Bmatrix} K_I^0(\pm a) + \sum_k \Delta K_I^k(\pm a) \\ K_{II}^0(\pm a) + \sum_k \Delta K_{II}^k(\pm a) \end{Bmatrix}$$

(17)

where and are the stress intensity factors without considering the interaction. As depicted in Eq. (18), they are

$$\begin{Bmatrix} K_I^0(\pm a) \\ K_{II}^0(\pm a) \end{Bmatrix} = \begin{Bmatrix} \sigma^\infty \cos^2 \beta \\ \sigma^\infty \sin \beta \cos \beta \end{Bmatrix}$$

(18)

In the study, considerations are made on the interaction of an arbitrarily located and oriented crack near a free-boundary. The test problems of rectilinear crack normal to the free boundary are evaluated for different geometric parameters of d/a. The integral of Eq. (14) and (15) are numerically evaluated with Gauss-Legendre quadrature rule. The number of discrete points on crack and semi-infinite plane are selected as 300 to secure the numerical accuracy. In addition, the integral from is truncated to an interval of. Results are shown in Table 1, good agreement meet with the singular integral approach of Cook and Erdogan [12]. However, the accuracy decreases for crack in close proximity to the free boundary. In the cases of slant crack approaching the free boundary, mode II effect turn out. As illustrated in Fig. (8)~(9), the interaction effect of crack and semi-infinite plane is enhanced for inner tip, and $K_{IA}(K_{IIA})$ is always greater than $K_{IB}(K_{IIB})$. In addition, mode I effect can be very perceptive in slant angle of $\beta \leq 40°$ for the close proximity between
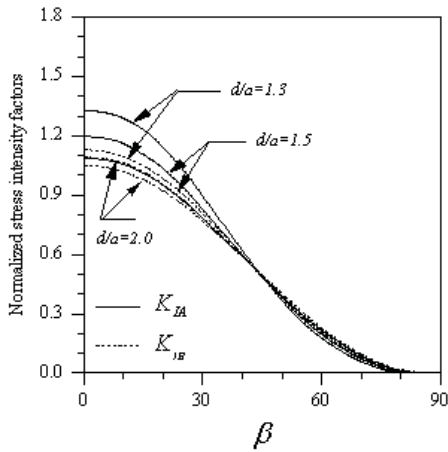
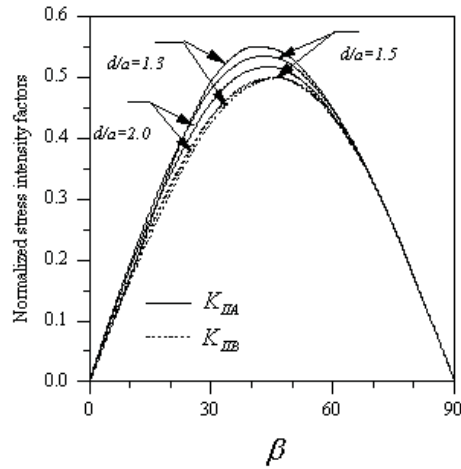Figure 8: Normalized K_I for different aligned crack interact with perpendicular free boundary

Figure 9: Normalized K_{II} for different aligned crack interact with perpendicular free boundary interact with perpendicular free boundary

crack and free edge. However, the sensitivity of close proximity effect in mode I lost for the aligned angle larger than $40°$, and the deviation between K_I and K_{II} are small. $K_{IB}(K_{IIB})$ retains the maximum value in the range of $30° \sim 45°$, nevertheless, the close proximity adjust the maximum value of stress intensity factor toward to the $30°$. Furthermore, there is no difference for $K_{IB}(K_{IIB})$ in $0° \sim 30°$ and $45° \sim 90°$ for any close proximity parameters (d/a). The alternating iteration may fail to converge for the cases of and . The reason for this trouble may result from the conventional numerical integration scheme to treat mathematical singularity unsatisfactorily. For close spaced singularities, thus the degree of polynomials in numerical integration must be increased radically to achieve reasonable numerical accuracy. Consequently, this insufficiency ceases this alternating method in cases of too close proximity problems.

Interactions of Two Equal Length Cracks

Similar approach is applied in the estimation for two cracks interaction. As denoted in Fig. (10), Büeckner superposition is employed again to separate the multi-domain into two single regions. Nevertheless, a modified alternating method was examined in the iteration calculation. The practice is simplified by using the averaged traction along the crack instead of averaged traction on the existing crack. The averaged traction for the kth iteration are simply integrated along the crack length. i.e., simplified iteration method, the traction on the imaginary site are assumed to be only reflected from the averaged traction on the existing crack. The averaged traction for the kth iteration are simply integrated along the crack length.

Table 1: Stress intensity factors for a rectilinear crack normal to a semi-infinite plane

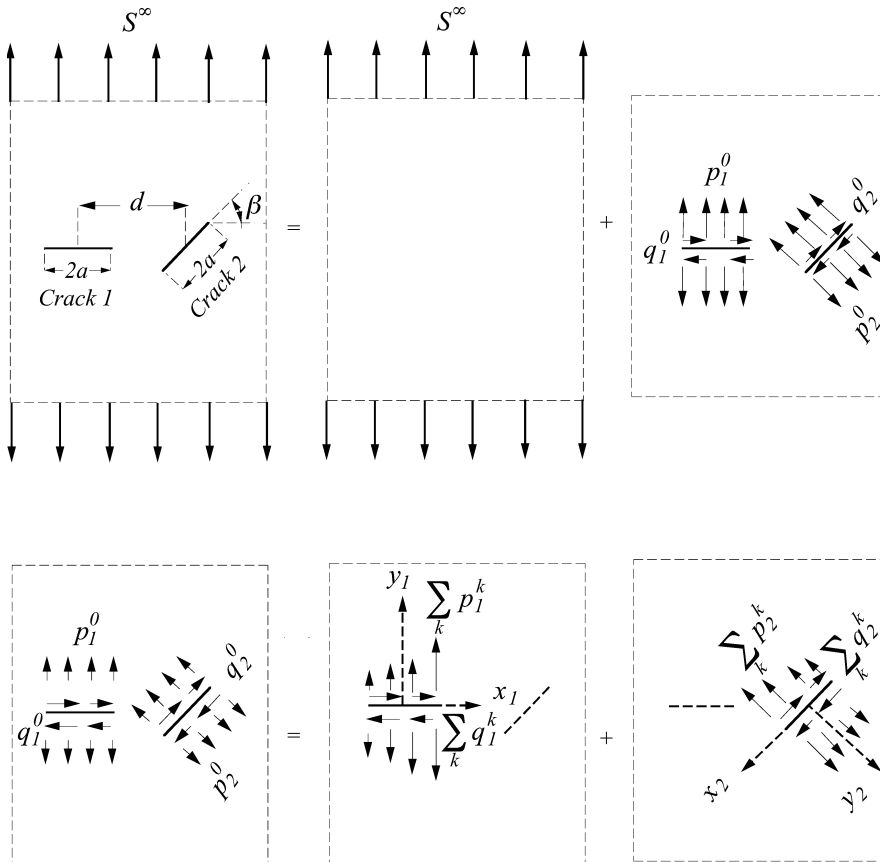|	Cook and Erdogan [12]		Present results	
$\frac{d}{a}$	$\frac{K_I(-a)}{\sigma^\infty\sqrt{\pi a}}K_I$	$\frac{K_I(a)}{\sigma^\infty\sqrt{\pi a}}K_{II}$	$\frac{K_I(-a)}{\sigma^\infty\sqrt{\pi a}}K_I$	$\frac{K_I(a)}{\sigma^\infty\sqrt{\pi a}}K_{II}$
1.01	1.330	3.720	1.326	3.465
1.05	1.254	2.159	1.255	2.282
1.10	1.211	1.759	1.210	1.769
1.15	1.183	1.575	1.182	1.573
1.20	1.163	1.464	1.161	1.461
1.25	1.146	1.388	1.145	1.385
1.50	1.097	1.204	1.095	1.201
2.00	1.054	1.091	1.052	1.089
5.00	1.009	1.011	1.006	1.008

Figure 10: Büeckner's superposition for the problem of two interacting cracks

i.e.,using an integral sequence of Gaussian-Legedre quadrature scheme in the alternation iteration. In this simplified iteration method, the traction on the imaginary site are assumed to be only reflected from the averaged traction on the existing crack. The averaged traction for the kth iteration are simply integrated along the crack length. i.e.,

The Westergaard functions [11] for a crack with averaged traction $(\hat{p})$ and $(\hat{q})$ can be assessed as

$$\begin{Bmatrix} \hat{p}_j^k \\ \hat{q}_j^k \end{Bmatrix} = \frac{1}{2a_j} \begin{Bmatrix} \int_{-a_j}^{a_j} p_j^k(x_j)dx_j \\ \int_{-a_j}^{a_j} q_j^k(x_j)dx_j \end{Bmatrix}, \quad j = 1,2 \tag{19}$$

averaged traction $(\hat{p})$ and $(\hat{q})$ can be assessed as

In the case of a polar coordinate system as referred to in Fig. 5, The stress distributions near the tip of a so called Griffith crack, which is loaded by a set of uniform normal and shear pressures ($\hat{p}$ and $\hat{q}$), could be derived from Eqs (19) and (20). However, the solution was also obtained using Fourier integral transform by Sneddon [10].The stress distributions ahead the tip of a pressurizing Griffith crack tip can be formulated as

$$\begin{Bmatrix} Z_I \\ Z_{II} \end{Bmatrix} = \begin{Bmatrix} \hat{p} \\ -i\hat{q} \end{Bmatrix} (\frac{z}{\sqrt{z^2 - a^2}} - 1) \tag{20}$$

to in Fig. 5, The stress distributions near the tip of a so called Griffith crack, which is loaded by a set of uniform normal and shear pressures ($\hat{p}$ and $\hat{q}$), could be derived from Eqs (19) and (20). However, the solution was also obtained using Fourier integral transform by Sneddon [10].The stress distributions ahead the tip of a pressurizing Griffith crack tip can be formulated as

$$\sigma_{yy}(r,\theta) = \hat{p}\left[-1 + A(r,\theta) - B(r,\theta)\right] + \hat{q}\left[2C(r,\theta) - D(r,\theta)\right]$$
$$\sigma_{xx}(r,\theta) = \hat{p}\left[-1 + A(r,\theta) + B(r,\theta)\right] + \hat{q}D(r,\theta) \tag{21}$$
$$\tau_{xy}(r,\theta) = \hat{p}D(r,\theta) + \hat{q}D\left[-1 + A(r,\theta) - B(r,\theta)\right]$$

where

$$A(r,\theta) = \frac{r}{\sqrt{r_1 r_2}} \cos\left(\theta - \frac{\theta_1 + \theta_2}{2}\right)$$

$$B(r,\theta) = \frac{ra^2}{(\sqrt{r_1 r_2})^3} \sin\theta \sin\frac{3(\theta_1 + \theta_2)}{2}$$

$$C(r,\theta) = \frac{r}{\sqrt{r_1 r_2}} \sin\left(\theta - \frac{\theta_1 + \theta_2}{2}\right) \tag{22}$$

$$D(r,\theta) = \frac{ra^2}{(\sqrt{r_1 r_2})^3} \sin\theta \cos\frac{3(\theta_1 + \theta_2)}{2}$$
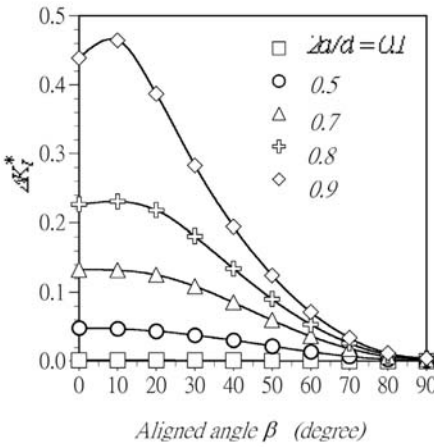
Figure 11(a): Variation of mode I intensity factors at the inner tip of crack-1 in Fig. 2
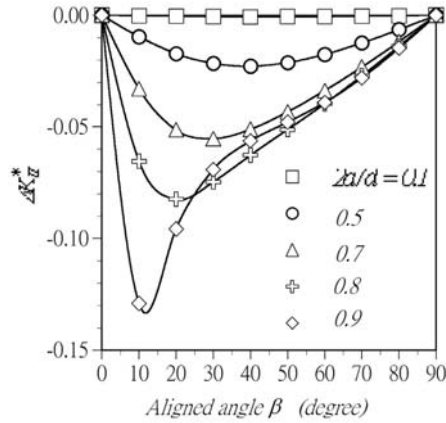
Figure 11(b): Variation of mode II intensity factors at the inner tip of crack-1 in Fig. 2

This modified model can significantly increase the computation efficiency in the iteration. The values of the stress intensity factors in this modified iteration method are accessed by Eq. (16) sequentially. Table 2 lists the iterated stress intensity factors for two identical collinear cracks which are arranged in different configurations. The error becomes noticeable for closely located cracks. This calculation error may be attributed to the highly non-linear interaction between cracks, which may destroy the linear average assumption as depicted in Eq. (19) in each iterative cycle.

Two oriented equal length cracks with different aligned angles, as shown in Fig. 10, are iterated by employing the proposed alternating iteration procedure. The changes in the stress intensity factors which are induced by the interaction of cracks, ΔK_I^* and ΔK_{II}^*, are evaluated as a specimen with different configurations. The results in Fig. 11(a) reveal that a strong interaction effect exists between cracks which are located closely. It also depicts that a smaller aligned angle β may introduce a stronger interaction effect on K_I^*. Fig. 11(b) shows that the induced ΔK_{II}^* at the inner tip of crack 1 is slightly conducted. A relative large variation of ΔK_{II}^* is found as the cracks are aligned with an angle β between $10° \sim 40°$. Calculated results indicate that the interaction effect on the mode II SIF is not such significant as it does on the mode I SIF. However, the interaction effect on K_{II}^* still can not be ignored as cracks are located closely. A high K_{II}^* could produce an out-of-plane growth for a straight crack, i.e., crack kinking. A similar variation of the ΔK_I^* was found at the inner tip of crack-2 as depicted in Fig. 12(a). The stress intensity factor K_I^* is enhanced for a slant angle of $\beta's$. The induced magnitude of ΔK_I^* at the inner
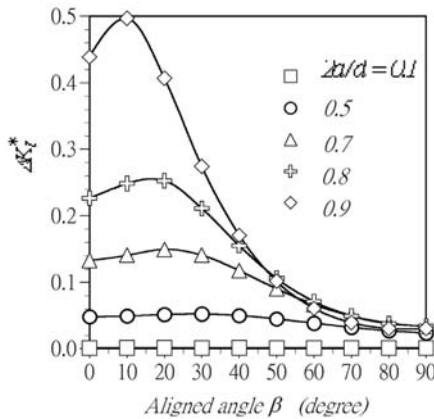
Figure 12(a): Variation of mode I intensity factors at the inner tip of crack-2 in Fig. 2
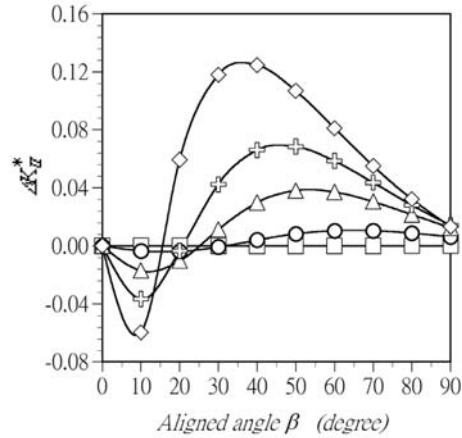
Figure 12(b): Variation of mode II intensity factors at the inner tip of crack-2 in Fig. 2

tip of crack-2 tends to be the greatest among those existing crack tips. Nevertheless, the sum of the up total stress intensity factors at the crack tips show that the inner tip of crack-1 may be the most suspicious fracture initiation site. The results in Fig. 12(b) delineate that the variation of ΔK_{II}^* at the inner tip of crack 2 is shielded for a smaller aligned angle case. However, the interaction between the cracks has only induced a little influence on the stress intensity factor K_{II}^*. A similar interaction effect on the outer crack tips of crack 1 and 2 is found. However, the induced ΔK_I^* and ΔK_{II}^* at the outer crack tips are far less than those induced at the inner tips. Results reveal that attention should be drawn to the inner tip of crack-1, because it is apt to fail in the mix oriented configuration. The stress intensity factor is enhanced for closely located cracks with an aligned angle in the range of $\beta = 0° \sim 20°$. The mode II condition is slightly induced for crack-1 by the alignment of crack-2.

Discussions and Conclusions

An alternating iteration method has been applied to calculate the stress intensity factors of a oriented crack when approaching the obstacle of straight crack or free boundary. Fair good agreements can be drawn if the interacting subjects are not in close nearness. However, conventional integration scheme using orthogonal polynomial expansion is not good enough to compensate the radical stress field increment for two approaching stress singularities. But the instinct nature of alternating iteration method for multiple connected domains is, nevertheless a good scheme to deal with interacting boundary problems in solid mechanics. As internal crack interacts with free boundary, mode I increase when crack approach the free semi-infinite plane, however, maximum mode II stress intensity factors shift to the

Table 2: Stress intensity factors for two collinear aligned cracks

	Stress Intensity Factors			
	Iteration method		Analytical method	
$2a/d$	with average traction		Tada's Handbook [13]	
	K_{IA}^*	K_{IB}^*	K_{IA}^*	K_{IB}^*
0.05	1.0003	1.0003	1.0003	1.0003
0.1	1.0012	1.0013	1.0012	1.0013
0.2	1.0046	1.0057	1.0046	1.0056
0.3	1.0102	1.0138	1.0102	1.0138
0.4	1.0179	1.0272	1.0179	1.0272
0.5	1.0279	1.0479	1.0280	1.0480
0.6	1.0409	1.0802	1.0409	1.0804
0.7	1.0577	1.1325	1.0579	1.1333
0.8	1.0806	1.2258	1.0811	1.2289
0.9	1.1159	1.4358	1.1174	1.4539
0.95	1.1455	1.7058	1.1490	1.7689

dimensionless stress intensity factors for the inner tip is K_{IA}^* and that for the outer tip is K_{IB}^*

lower angle from its original extreme of aligned angle . Mis-oriented dual-crack problems were also investigated with average traction reflecting simplification in this alternating iteration method. Results indicate that the accuracy of this modified alternative iteration method is dependent on the distance between the cracks. Close proximity may delimit the accuracy of the elastic interaction between cracks.

Acknowledgement

References

1. Sih, G. C. edited (1973). Mechanics of Fracture. Noordhoff International Publishing, Leyden.

2. Mikhlin, S. G. (1964). Integral Equations, Pergamon Press, Oxford.

3. Mura, T., Micromechanics of Defects in Solids, 2nd ed., Martinus Nijhoff, Boston, Mass., 1987

4. Hori, M., and Nemat-Nasser, S., Interacting Micro-cracks Near the Tip in the Process Zone of a Macro-crack, J. Mech. Phys. Solids, Vol.35, pp. 601-629, 1987

5. Isida, M., Method of Laurent Series Expansion for Internal Crack Problems, Mechanics of Fracture, Vol. I (Edited by G. C. Sih), Noordhoff International

Publishing, Leyden, pp. 56-129, 1973

6. Isida, M and Noguchi, H., Arbitrary Array of Cracks in Bonded Half Planes Subjected to Various Loadings, Engng. Fracture Mech., Vol.46, pp. 365-380, 1993

7. Gupta, G. D. and Erdogan, F., The Problem of Edge Cracks in an Infinite Strip, J. App. Mech., Vol.41, pp. 1001-1006, 1974

8. Hills, D. A., Kelly, P. A., Dai, D. N., and Korsunsky, A. M., Solution of Crack Problems: The Distributed Dislocation Technique, Kluwer Academic Publisher, Dordrecht, the Netherlands, 1996

9. Kantorovich, L. V. and Krylov, V. I., Approximate Methods of Higher Analysis. Interscience, New York, 1964

10. Sneddon, I. N. and Elliot, H. A., The Opening of a Griffith Crack under Internal Pressure. Q. Appl. Math., Vol.4, pp. 262-267, 1964

11. Sokolnikoff, I. S., Mathematical Theory of Elasticity, 2nd ed., MacGraw-Hill, New York, 1956

12. Cook, T. S. and Erdogan, F., Stress in Bonded Materials with a Crack Perpendicular to the Interface, Int. J. Engng. Sci., Vol.10, pp. 677-697, 1972

13. Tada, H., Paris, P. C., and Irwin, G. R., The Stress Analysis of Cracks Handbook, 2nd edition, Paris Productions Incorporated (and Del Research Corporation), 1985